Thermochemical storage: first results of pilot storage with moist air

Foivos MARIAS[1], Gwennyn TANGUY[1*], Jöel WYTTENBACH[1], Sylvie ROUGE[1], Philippe PAPILLON[1]

[1] CEA / LITEN / INES, Le Bourget du Lac (France)

* Corresponding author: gwennyn.tanguy@cea.fr

Abstract

The laboratory of Thermal systems at CEA-INES works on seasonal storage of solar thermal energy for household applications. Thermochemical storage has been adopted and hydration/dehydration reactions of inorganic salts are being used. The objective of this work is to evaluate the feasibility of a significant scale thermochemical storage system operating under conditions as close as possible to reality. Complete hydration/dehydration cycles have been performed using moist air both as reactive and heat transfer vector. The present paper presents the experimental setup, an energy analysis, theoretical assumptions on thermochemical storage and the first results of storage.

Keywords: thermochemical heat storage, chemisorption, salt hydrate, moist air, solar thermal.

Nomenclature

P [Pa]	Pressure;	ν	Stoichiometric coefficient;
P_{ref} [Pa]	Pressure of reference;	ΔH_r [J/mol]	Enthalpy of reaction;
P_v [Pa]	Partial water vapour pressure;	ΔS_r [J/K·mol]	Entropy of reaction;
T [K]	Temperature;	ΔP [Pa]	Pressure drop through the reactor;
r [$kg_{water}/kg_{dry\ air}$]	Moisture content-absolute humidity;	X	Advancement of reaction;
$r_{out\_reactor}$[$kg_{water}/kg_{dry\ air}$]	Moisture content-absolute humidity at the outlet of the reactor;	A [m^2]	Surface of the reactor;
		$r_{in\_reactor}$ [$kg_{water}/kg_{dry\ air}$]	Moisture content-absolute humidity at the intlet of the reactor;
Hr [%]	Relative humidity;		
M_{vap}= 0.018 [kg/mol]	Water vapour molar mass;	h_{vap} [$J/kg_{of\ water\ vapor}$]	Water vapour enthalpy;
$H_{wet\_air\_in}$ [J/ $kg_{of\ dry\ air}$]	Enthalpy of moist air in the inlet of the reactor;	t [s]	Time;
		$\dot{U}_{salt}$ [W]	Time variation of the internal energy of the salt;
$H_{wet\_air\_out}$ [J/ $kg_{of\ dry\ air}$]	Enthalpy of moist air in the outlet of the reactor;	$\dot{m}_{vap\_in}$ [$kg_{of\ water\ vapor}$/s]	Water vapour mass flow in the inlet of the reactor;
H_{wet_air} [J/ $kg_{of\ dry\ air}$]	Enthalpy of moist air;		
H_{dry_air} [J/ $kg_{of\ dry\ air}$]	Enthalpy of dry air;	$\dot{m}_{vap\_out}$ [$kg_{of\ water\ vapor}$/s]	Water vapour mass flow in the outlet of the reactor;
ΔH_{wet_air} [J/ $kg_{of\ dry\ air}$]	Difference of enthalpy of moist air between the inlet and the outlet of the reactor;		
$\dot{m}_{dry\_air}$ [$kg_{of\ dry\ air}$ /s]	Dry air mass flow;	$P_{\_th\_m}$ [W]	Thermochemical power calculated on mass evolution;
$P_{\_th\_water}$ [W]	Thermochemical power calculated on humidity of air;	$P_{\_th\_wet\_air}$ [W]	Thermochemical power calculated on enthalpy measurement in moist air;
R = 8.314 [J/K·mol]	Ideal gas constant;		
L [m]	Height of the bed;	T_2=$T_{wet\_air\_out}$	Temperature of moist air in the outlet of the reactor;
T_1=$T_{wet\_air\_in}$	Temperature of moist air in the inlet of the reactor;	m [kg]	Mass;

1. Introduction

The use of solar energy is a key element to achieve the target of 3x20 on European energy policy. Especially, household applications of solar energy have a particular interest as approximately 33% of final energy in Europe is used for household applications such as domestic hot water preparation and space heating [ESTIF]. Furthermore, lots of studies show [Hongois et al. 2008, Tanguy et al. 2009] that summertime solar energy surplus is enough to satisfy household thermal energy demand.

Consequently, seasonal storage seems to be the only way to achieve high solar fractions and reduce greenhouse gas emissions due to household applications.

A seasonal storage system designed to be used in household applications must satisfy at least the two following scientific constraints: 1) thermal losses between summertime and winter time must be reduced at a minimum level, 2) the volume of the storage system has to be as small as possible in order to be adapted for residential use, or in other terms a high energy density storage technique is required. Energy density of thermochemical storage can be up to ten times higher to the one of water. Moreover, thermochemical storage presents no thermal losses during storage phase because heat is stored in form of chemical potential. Taking into account these considerations, thermochemical storage seems to be the most appropriate solution for seasonal storage.

According to [Tanguy et al. 2009, Tanguy et al. 2010] a thermochemical system needs around 5-10 tons of solid material. A power of 2-4 kW should be provided by the reactor. A lot of, very interesting, experimental setups on that domain presented up to now are using small quantities of salts [Bertsch et al. 2009], with small output powers (inferior to 0.5 kg and 8 W) [Hongois et al.. 2010]. The first up scaled reactor was presented by ECN (3.6 kg) [Zondag et al. 2010a, Zondag et al. 2011].

The goal of this work is to evaluate the feasibility of a significant scale thermochemical storage system operating under conditions as close as possible to reality. Furthermore, a critical point for thermochemical storage systems is the stability of materials through time and their ability to provide stable performances for a long period (15 to 30 years at least). This is a very important parameter in order to evaluate investment costs [Zondag et al. 2010b] and to convince industrial partners and consumers of payback interest of that technology. A second goal of this paper is to examine stability of thermochemical material after several reaction cycles and their ability to provide constant performances through time.

2. Reaction

Thermochemical storage uses the heat of reversible endothermic/exothermic reactions in order to store heat. The general form of such a reaction is the following one:

$$A + B \leftrightarrow C + \text{heat}$$

The choice of the reaction is a crucial point on thermochemical storage. That choice is conditioned by the following considerations: 1) temperature of endothermic reaction must be compatible with the available solar field and with the type of solar collectors used; 2) temperature of the exothermic reaction must be in phase with the thermal application to fulfil; 3) separation of reactants have to be performed easily; 4) sanitary and environmental risks have to be taken into consideration.

Among all the potential reactions, taking into account that our goal is to develop a household system, which implicates specific sanitary constraint, and since flat plate collectors are supposed to be used, the choice of hydration/dehydration reactions of inorganic salts has been adopted. It consists in reversible solid (S2)-solid (S1)/ gas (G) reaction (also called chemisorption) [K. Edem N'Tsoukpoe et al. 2009] of the following general form:

$$S_1 + \nu \cdot G \leftrightarrow S_2 + \Delta H_r$$

These reactions present a mono-variant equilibrium between the hydrate and the dehydrate form of the reactive. The equation linking pressure to temperature for such a case is:

$$\ln (P_v/P_{ref}) = -\Delta H_r/RT + \Delta S_r/R$$

Both exothermic and endothermic reaction temperature depend on partial water vapour pressure and on equilibrium's position.

A lot of research teams work on the selection of reactive material. Many different reactions have been proposed [van Essen et al. 2009a, van Essen et al. 2009b, Bertsch et al. 2009, Kerskes et al. 2010, Hongois et al. 2008, Hongois et al. 2011]. Our study focuses mainly on the reactor and less on material selection. For those reasons, we chose to use aluminium potassium sulphate 12-hydrate ($KAl(SO_4)_2.12H_2O$), purity > 99%. Physical and chemical characteristics of that material are not so good in comparison to other materials [Table 1]; however it presents very few sanitary risks and this is the main raison of our choice in this first step. A first series of tests are performed with this salt in order to confirm our methodology, afterwards further tests are going to be carried out with other reactive materials more adapted to our case.

Table 1 : Material comparison characteristics.

Reaction	$KAl(SO_4)_2$ (3/12)	$MgSO_4$ (1/7) [van Essen et al. 2010]	$Al_2(SO_4)_3$ (5/18) [van Essen et al. 2010]	$MgCl_2$ (2/6) [van Essen et al. 2010]	$CaCl_2$ (0/2) [van Essen et al. 2010]
Energy density (kWh/m^3)	409	686	600	589	400

Our project partner, PROMES-CNRS investigated this reaction. According to PROMES there are two different hydrates, a 12-hydrate and a 3-hydrate. The reaction between the 12-hydrate and the 3-hydrate aluminium potassium sulphate is being used. The equilibrium curve of twelve- to three-hydrate superimposed to psychometric charts is given in [Figure 1] (red curve).

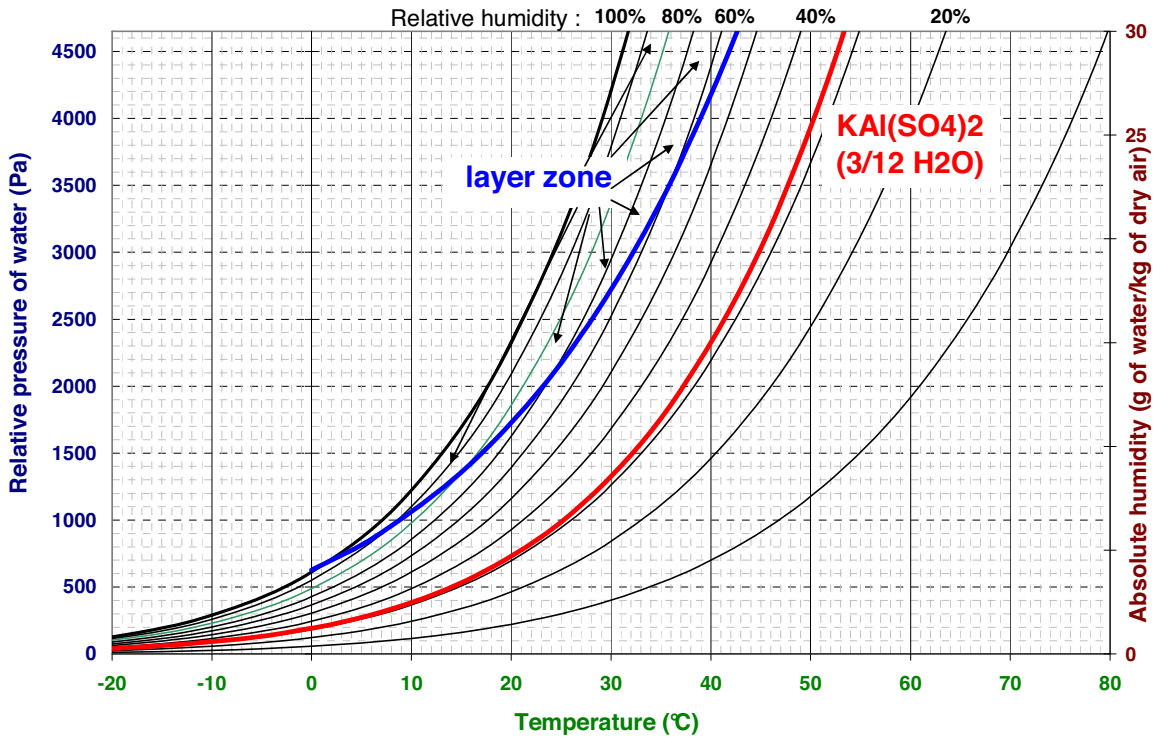

Figure 1 : Equilibrium curve and layer zone in moist air diagram

The maximum difference of temperature (elevation for exothermic reaction or decrease for endothermic reaction) that is induced by thermochemical reactions depends on two parameters: 1) the position of the equilibrium curve of the reaction and 2) on the inlet airflow conditions (temperature and partial water vapour pressure). According to the deviation from equilibrium, the difference of temperature induced by the reaction is more or less important.

Moreover, another phenomenon, which should be taken into consideration, is the formation of a hard impermeable layer observed in some hydration reactions [Rambaud 2009, van Essen et al. 2010, Zondag et al. 2010a]. [Zondag et al. 2010a] explains that phenomenon is due to an overhydration of the reactive salt during hydration reaction. PROMES and [Rambaud 2009] also gave a theoretical explication of that phenomenon. The formation of that hard impermeable layer takes place only in some hydration reactions, depending on particular temperature (T) and partial water vapour pressure (P_v) conditions. Under these P_v, T conditions during hydration reaction, water vapour presence is so important that it leads to the formation of a saturated solution which results to the formation of this hard impermeable layer observed. For the case of aluminium sulphate hydrate, we estimated the area of danger, noted as "layer zone" on [Figure 1].

3. Experimental setup and measurement

The experimental set up is composed, in series, of two air filters on the circuit inlet, a fan , a heating coil, a humidifier, the reactor and two air filters on the circuit outlet. A schematic diagram of the experimental setup is provided in [Figure 2]. Indoor air at 20°C is being used. An integrate, packed bed reactor containing an important quantity of salt (25 kg) is used, covering a square surface reactor of 0.64m². The packed bed has a height of 40mm; the porosity of the bed is around 42% and the energy density of the hydrated bed around 240 kWh/m^3. The reactor has been designed so that airflow is as uniform as possible through the reactor.

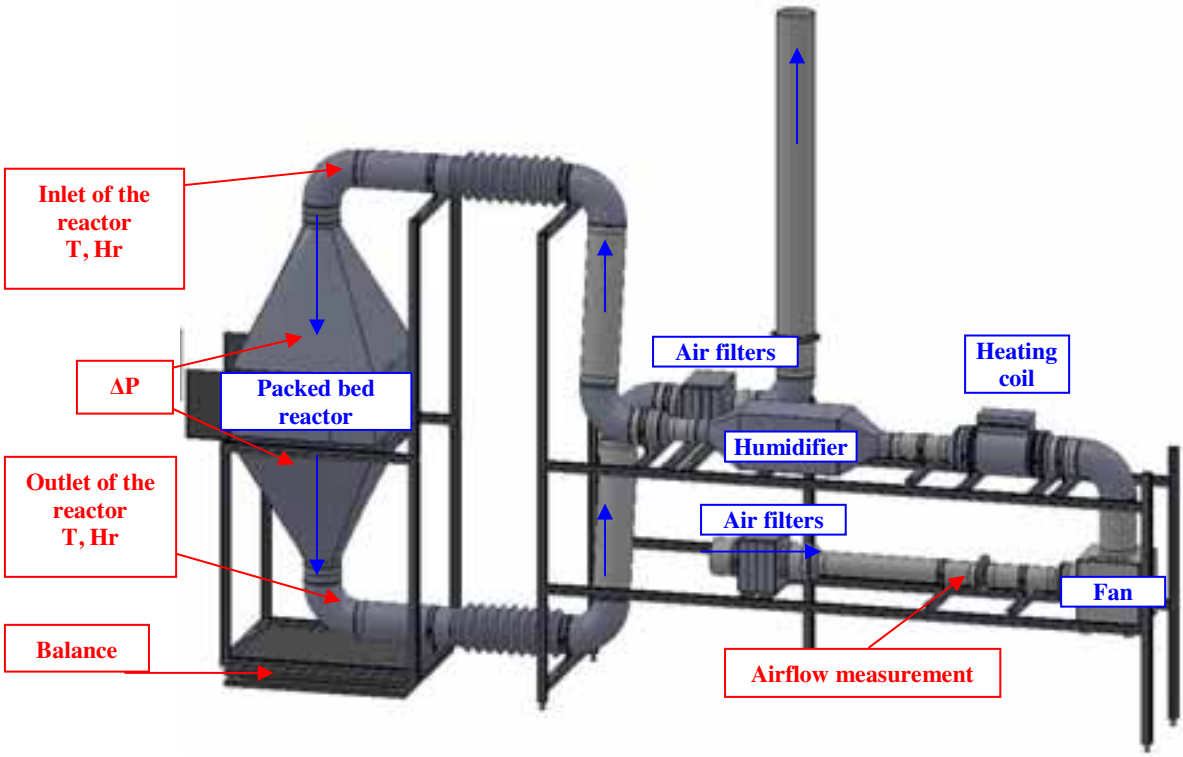

Figure 2 : Schematic presentation of the experimental setup.

The data measured are listed here below:

- Airflow temperature at the inlet and the outlet of the reactor, using PT100 sensors calibrated to 0.1K;
- Airflow temperature inside the reactor [Figure 3], using J-type thermocouples calibrated to +/-0.2 K;
- Inlet and outlet airflow humidity using two capacitive moist sensors (HUMICHIP, 17205 HM, VAISALA);
- Pressure drop over the reactor, using a pressure transmitter of an accuracy +/-0.5% of reading value +/-1 Pa;
- Reactive mass evolution using an 100g accurate balance (5000 series, VFP/VFS-600, OHAUS).

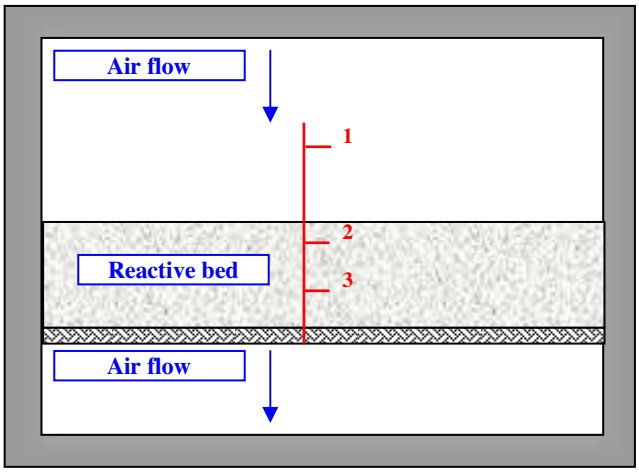

Figure 3 : Temperature measurement inside the reactor.

4. Operating conditions

Our goal is to study the feasibility of a thermochemical storage system operating under realistic conditions. Since such a system operates with moist air, outdoors temperature and relative humidity are two crucial parameters. A studied carried out to climate data in the case of France give us the following result:

- Outdoor conditions during non-heating period (summer and a part of autumn and spring):
  T= 20 to 40°C ; r= 10-20 $g_{water}/kg_{dry\ air}$
- Outdoor conditions during heating period (winter and a part of autumn and spring):
  T= -8 to 20°C ; r= 1-10 $g_{water}/kg_{dry\ air}$

The experimental setup is designed so that test can be operated in conditions as close as possible to realistic outdoor conditions.

For all the tests presented in this paper, indoor air was blew in at a flow rate of 150m^3/h and a temperature of 20°C.

4. 1. Dehydration conditions

Operating conditions at the reactor inlet during dehydration mode were: T=65°C and r=indoor air absolute humidity.

4. 2. Hydration conditions

Some studies [Tanguy et al. 2010] show that hydration reaction rate is limiting in comparison to dehydration. After air treatment, operating conditions at the reactor inlet, for all hydration tests were: a temperature of T=15°C and an absolute humidity of r=7-8 $g_{water}/kg_{dry\ air}$. These conditions are situated out of the "layer zone".

5. Experimental results and discussions

5. 1. Energy balance

A crucial point for thermochemical storage is to be able to provide the power demanded by the heating system. Thermochemical power was calculated during the tests carried out, according three independent methods presented below. The analysis is performed only for stationary operation of thermochemical storage; it does not take into consideration transitory phases.

The system is composed of the reactive salt and moist air. Exothermic reaction is induced by the consumption of water vapour contained into moist air, and the heat is released into the air. Moist air has then a double role: it transports one of the reactive elements (water vapour) and at the same time it transfer heat.

During endothermic reaction, again, moist air both transports the heat needed for he dehydration of the salt and evacuates the water vapour released by the reaction.

A schematic representation of that energy analysis is given in [Figure 4, Figure 5]. The corresponding equations for both hydration and dehydration reactions are the following ones:

For the reactive salt:

During dehydration reaction:

$$\dot{U}_{salt} = (\dot{m}_{vap\_in} - \dot{m}_{vap\_out}) \cdot (h_{vap}(T) - \Delta H_r / M_{vap}) = dm/dt \cdot (h_{vap}(T) - \Delta H_r / M_{vap}) \quad [W]$$

During hydration reaction:

$$\dot{U}_{salt} = (\dot{m}_{vap\_in} - \dot{m}_{vap\_out}) \cdot (\Delta H_r / M_{vap} - h_{vap}(T)) = dm/dt \cdot (\Delta H_r / M_{vap} - h_{vap}(T)) \quad [W]$$

For the reactor and moist air:

$$\dot{m}_{dry\_air} \cdot (H_{wet\_air\_out} - H_{wet\_air\_in}) = -\dot{U}_{salt} \quad [W]$$

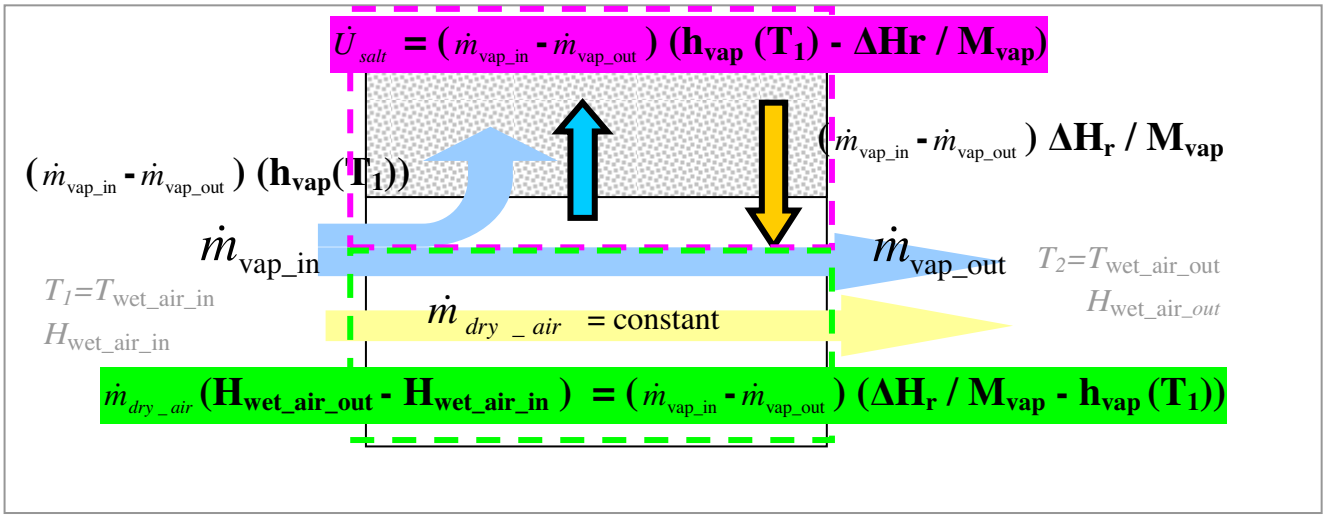

Figure 4 : Energy analysis for hydration reaction.

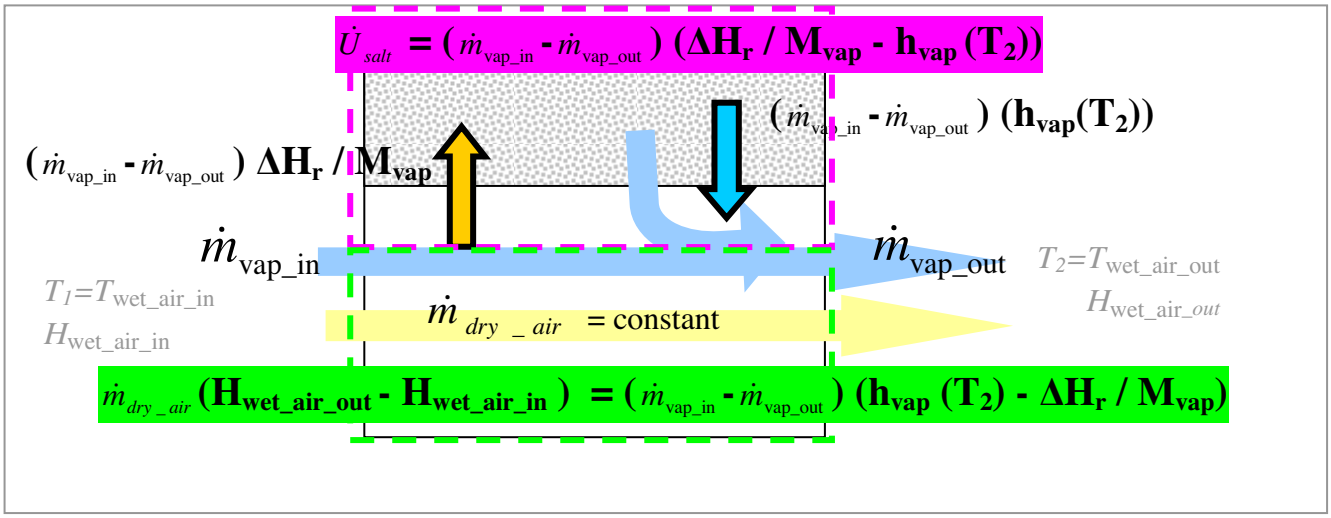

Figure 5 : Energy analysis for dehydration reaction.

Enthalpy of wet air is given by the enthalpy of dry air plus the enthalpy of water vapour contained into moist air: $H_{wet\_air} = H_{dry\_air}(T) + r \cdot h_{vap}(T)$. Enthalpy of both dry air and water vapour depend on temperature. One can calculate them using the following equations [ASHRAE 1997]:

$$H_{dry\_air} = 1.3478 \cdot 10^{-4} \cdot T^3 + 7.15357 \cdot 10^{-3} \cdot T^2 + 1005.8281 \cdot T$$

(precision: +/-0.032% for T=-25°C to +100°C; for T in [°C] in that case)

$$h_{vap} = -1.004088 \cdot T^2 + 1851.974 \cdot T + 2500770$$

(precision:+/-0.022% for T=-25°C to +90°C; for T in [°C] in that case)

We also suppose that enthalpy of reaction is independent of temperature.

The thermochemical power may be defined as the power released by the exothermic reaction or needed for the endothermic reaction. It takes into account the variation of internal energy of the salt and the enthalpy of water, which is released (during dehydration reaction) or consumed (during hydration reaction). This is thermal power and it can be evaluated either:

- by measuring the evolution of mass of the reactive salt (Equation 1);
- from the quantity of water consumed (hydration) or released (dehydration) during a reaction (Equation 2);
- by enthalpy measurement in moist air (Equation 3).

The corresponding equations in order to calculate thermochemical power for both exothermic and endothermic reactions are the following ones:

For both hydration and dehydration reactions:

$$P_{th\_m} = \frac{dm}{dt} \cdot \frac{\Delta H_r}{M_{vap}} \qquad \text{[Equation 1]}$$

$$P_{th\_water} = \dot{m}_{dry\_air} \cdot (r_{in\_reactor} - r_{out\_reactor}) \cdot \frac{\Delta H_r}{M_{vap}} \qquad \text{[Equation 2]}$$

For hydration reaction:

$$P_{th\_wet\_air} = \dot{m}_{dry\_air} .(\Delta H_{wet\_air} + (r_{in\_reactor} - r_{out\_reactor}) \cdot h_{vap}(T_1)) \qquad \text{[Equation 3a]}$$

For dehydration reaction:

$$P_{th\_wet\_air} = \dot{m}_{dry\_air} .(-\Delta H_{wet\_air} + (r_{in\_reactor} - r_{out\_reactor}) \cdot h_{vap}(T_2)) \qquad \text{[Equation 3b]}$$

5. 2. Dehydration – Endothermic reaction results

The main criterion indicative of the stability of the reacting materials is the advancement of the reaction (X). X can be defined as the ratio of the quantity of salt reacted over the maximum theoretical quantity of salt that can react. [Figure 6] shows the evolution of X through the different cycles operated under the conditions mentioned previously. One can remark an excellent reproducibility of reaction through time except dehydration test number 7. An explication of this difference is given in part [*5. 5.*].

Another important design element for a thermochemical storage system is the pressure drop through the reactor [Figure 6]. A constant airflow of 150m^3/h was regulated during the reaction. The pressure drop (ΔP) through the reactor decreases more and more slowly during a dehydration reaction up to steady state at the end of the cycle. After each cycle, the maximal level of pressure drop decreases.

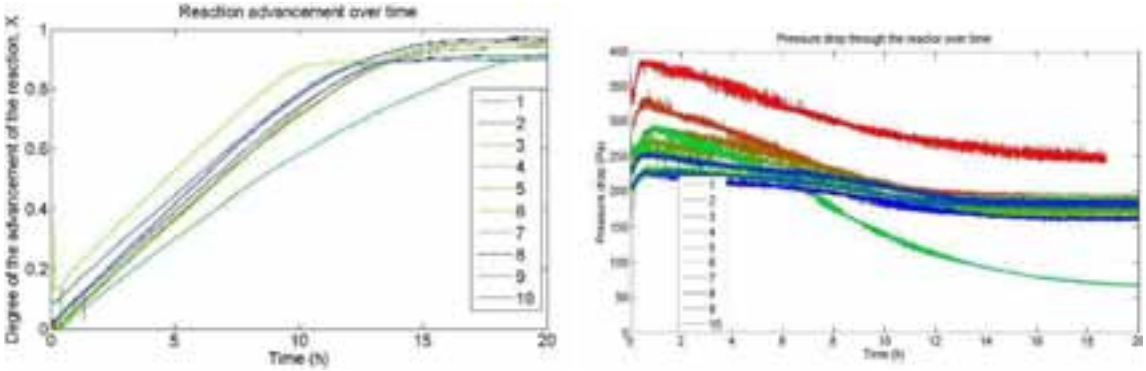

Figure 6: Left: Advancement of dehydration reaction; - Right: Pressure drop through the reactor during dehydration reaction.

Temperature evolution through the reactive salt over time is given in [Figure 7]. This is the result for one dehydration reaction. Similar results were observed for all dehydration tests. An important deviation from equilibrium leads to a rather important difference of temperature.

Thermochemical power is also calculated based on the analysis presented in part [*5. 1.*] [Figure 7]. By convention thermochemical power calculated by the three methods is consider being positive. We can remark that the three curves representing thermochemical power have the same form, which is an encouraging result.

On the other hand one can also remark important differences on the values calculated by the three methods. The green curve was calculated by the quantity of water released during dehydration reaction ($P_{th\_water} = \dot{m}_{dry\_air} \cdot (r_{in\_reactor} - r_{out\_reactor}) \cdot \frac{\Delta H_r}{M_{vap}}$ [Equation 2]), using capacitive moist sensors. However, capacitive moist sensors are not accurate when the air flow is rather hot (60°C for instance), which is the case during dehydration reaction. So, we believe that this measure is not very accurate.

The red curve estimated by measurement in wet air ($P_{th\_wet\_air} = \dot{m}_{dry\_air} .(-\Delta H_{wet\_air} + (r_{in\_reactor} - r_{out\_reactor}) \cdot h_{vap}(T_2))$ [Equation 3b]) is calculated using both PT100 and capacitive moist sensors. But, as important thermal gradient inhomogeneities were observed, combined with the previous remark on accuracy of capacitive moist sensors on that region of temperatures, we think that this measure is not very accurate.

The blue curve was calculated by measuring the evolution of mass of the reactive salt ($P_{th\_m} = \frac{dm}{dt} \cdot \frac{\Delta H_r}{M_{vap}}$ [Equation 1]). The total mass evolution is about 8kg, while the accuracy of the balance is 100g. On our point of view, this measure is the more accurate concerning the thermochemical power evaluation.

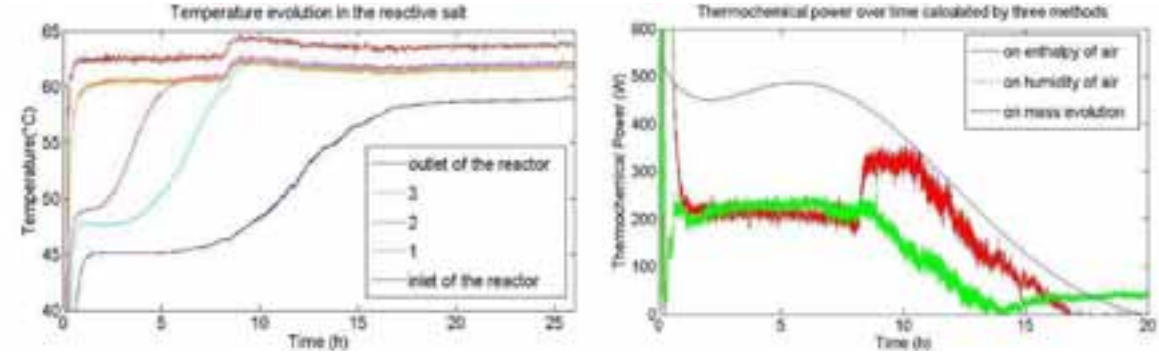

Figure 7: Left: Temperature evolution in the reactive salt; - Right: Thermochemical power over time calculated by three methods.

5. 3. Hydration – Exothermic reaction results

Advancement of reaction over time is plot in [Figure 8]. Due to regulation difficulties of the humidifier, hydration reactions were less regular than hydration ones. Nevertheless, one can remark a very good reproducibility except hydration test number 7. An explication of this difference is given in part [*5. 5.*].

The pressure drop during the reaction is given in [Figure 8]. A constant airflow of 150m^3/h was imposed during the reaction. Pressure drop through the reactor increases steadily during each hydration cycle up to a stable value. After each cycle, the level of pressure drop decreases.

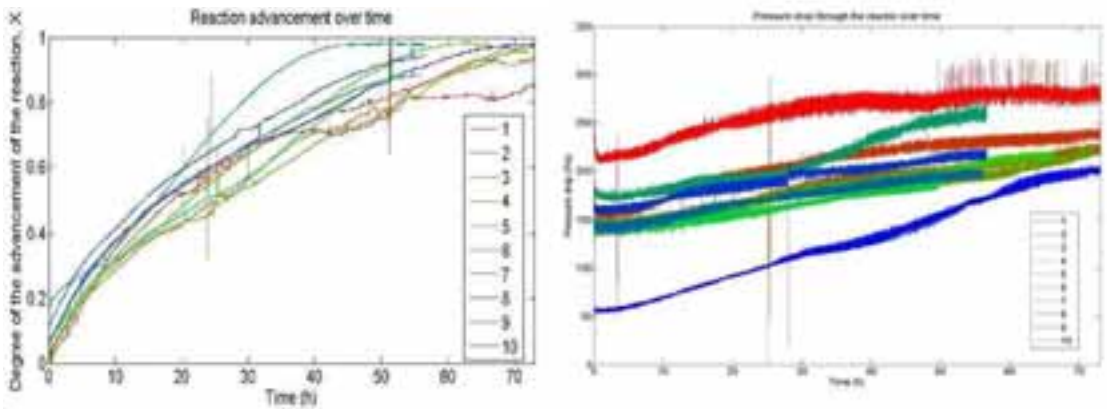

Figure 8: Left: Advancement of hydration reaction; - Right: Pressure drop through the reactor during hydration reaction.

Temperature evolution through the reactive salt over time is given in [Figure 9] for one hydration test. Similar results were observed for all hydration tests. The presence of a reaction front is observed. The elevation of temperature induced by the exothermic reaction is not very important. This is not a surprising result since the operating conditions for hydration and the position of the equilibrium leads to a little deviation from equilibrium.

Power extracted by exothermic reaction is also measured [Figure 9]. By convention thermochemical power calculated by the three methods is consider being positive. The three curves calculating thermochemical power have, once again, the same form. Moreover, for hydration test the three ways to calculate thermochemical power converge much better. At those conditions of temperature and relative humidity capacitive moist sensors perform much better and very few thermal gradient inhomogeneities are observed. Nevertheless, for the reasons explained in the former paragraph, the most accurate way to evaluate thermochemical power remains the mass evolution of reactive salt.

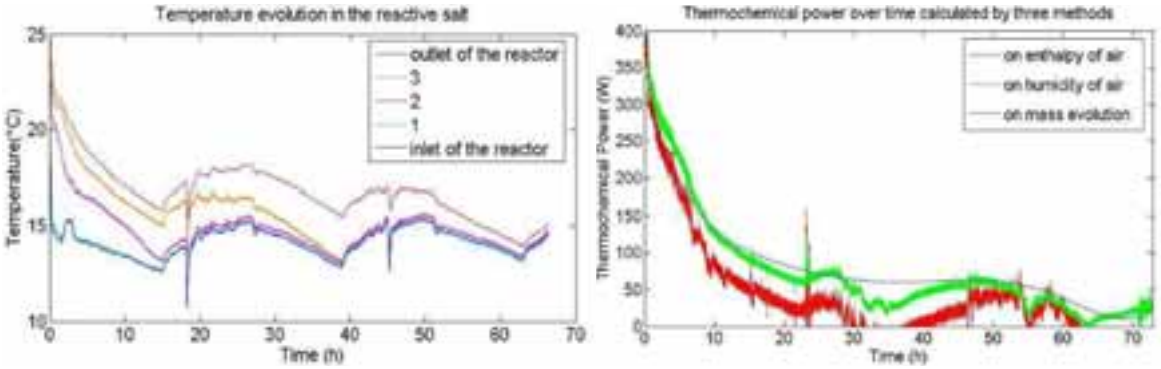

Figure 9: Left: Temperature evolution in the reactive salt; - Right: Thermochemical power over time calculated by three methods.

5. 4. Volume evolution

During each hydration/dehydration cycle, a variation of the volume of the salt has been observed. It is demonstrated by a variation of the thickness of the salt [Figure 10]. The same observation was pointed out by [Rambaud 2009, van Essen et al. 2010]. This variation was not measured but it can be estimated around 20-30% of the initial thickness (in our case).

Figure 10 : Left: Height of the bed at the end of hydration reaction; - Right: Height of the bed at the end of dehydration reaction.

5. 5. Tests in the "layer zone"

As mentioned before, hydration test 7 and dehydration test 7 present different performances in comparison to all the other hydration/dehydration cycles. During the 7th hydration test, relative humidity was Hr=90% due to a problem with the humidifier controller. The conditions of that test were in consequence inside the "layer zone" inducing the formation of a layer [Figure 11], which explains a faster evolution of X [Figure 8] together with increased pressure drop compared with previous hydration tests [Figure 8].

Figure 11: Formation of the top layer.

The following dehydration test (dehydration number 7) took place at the same conditions as all dehydration tests. One can notice that X increases slower [Figure 6] than in the other tests. Moreover, the pressure drop through the reactive salt decreases sharply [Figure 6]; the explanation being that the volume reduction of the salt broke the layer.
Furthermore, performances measured during the following cycles showed similar results to the ones before the formation of the layer [Figure 6, Figure 8]. This is a very encouraging observation. It proves that, for our experimental configuration, the formation of the layer does not induce any major problem. It can be explained because the height of the bed is L= 40mm and the surface is A=0.64m^2 it, gives a ratio A/L=160. In the experimental setup of ECN [van Essen et al. 2010, Zondag et al. 2010a], this ratio (A/L) is much smaller, so the formation of the layer can cause more difficulties.

6. Conclusions

This paper presents the experimental setup, an energy analysis and some theoretical assumptions on thermochemical storage. Moreover, the first results obtained are presented. As far as it concerns future work, improvements have to be done to the experimental setup. More tests are going to be operated with other reactive salts, more adapted than the one used here for household activities. Moreover, we work on the intensification of heat and mass transfer through the reactor.

It is important to outline the good stability of the reactive material after several cycles which leads to a very good reproducibility of the results, even if a cycle led to a top layer. This is a very important observation for the future of thermochemical storage systems. Interesting level of thermochemical power was also measured. Moreover, the problem of the formation of a hard layer is discussed. The results obtained show that for this experimental configuration the formation of the layer is not a major problem. We believe that those results constitute a first feasibility study of a significant scale thermochemical storage system operating under realistic conditions.

These results are very encouraging and they prove that thermochemical energy storage is not only necessary but also a realistic technological solution even if the economical evaluation of a large scale production of such a system is not done yet.

Acknowledgements

To our project partners PROMES-CNRS that provide us the information about the reactive material.
This research, included in the “Solaire Duo” project is funded by OSEO. The authors gratefully acknowledge this support.

References

ASHRAE, 1997. ASHRAE Fundamentals Handbook (SI), CHAPTER 6 PSYCHOMETRICS, 1997.

Bertsch, F., Mette, B., Asenbeck, B., Kerskes, H., Müller-Steinhagen, H., 2009. Low temperature chemical heat storage – an investigation of hydration reactions; presented at Effstock 2009

ESTIF; Weiss, W., Biermayr, P.,. Potential of solar thermal in Europe, ESTIF.

Hongois S, Stevens P, Coince A-S, Kuznik F, Roux J-J, 2008. Thermochemical storage using composite materials; presented at Eurosun 2008.

Hongois, S., Kuznik, F., Stevens, P., Roux, J.-J., Radulescu, M., Beaurepaire, E., 2010. THERMOCHEMICAL STORAGE USING COMPOSITE MATERIALS: FROM THE MATERIAL TO THE SYSTEM; presented at Eurosun 2010.

Hongois, S., Kuznik, F., Stevens, P., Roux, J.-J., 2011. Development and characterisation of a new MgSO4 – zeolite composite for long-term thermal energy storage. Solar energy materials and solar cells, 95 (2011), 1831-1837.

K. Edem N'Tsoukpoe, Hui Liu, Nolwenn Le Pierrès, Lingai Luo, 2009. A review on long-term sorption solar energy storage. Renewable and Sustainable Energy Reviews, 13, (2009), 2385–2396.

Kerskes H., Mette B., Asenbeck S., Drück H., Müller-Steinhagen H., 2010. EXPERIMENTAL AND NUMERICAL INVESTIGATIONS ON THERMO-CHEMICAL HEAT STOARGE; presented at Eurosun 2010.

RAMBAUD Guillaume, 2009. Problématique des transferts en milieu poreux réactif déformable pour procédés de rafraichissement solaire. PhD Thesis, PROMES-CNRS, UNIVERSITE DE PERPIGNAN, 2009.

Tanguy, G., Papillon, P., Paulus, C., 2009. SOLAR COMBISYSTEMS AND STORAGE: THE WAY TO ACHIEVE HIGH SOLAR FRACTION; presented at IRES 2009.

Tanguy, G., Papillon, P., Paulus, C., 2010. Seasonal storage coupled to solar combisystem: dynamic simulations for process dimensioning; presented at Eurosun 2010.

van Essen, V.M., Cot Gores, J., Bleijendaal, L.P.J., Zondag, H.A., Schuitema, R., Bakker, M., van Helden, W.G.J., 2009a. Characterization of MgSO4 hydrate for thermochemical seasonal heat storage. Journal of solar energy engineering, Vol.131, November 2009.

van Essen, V.M. ; Bleijendaal, L.P.J.; Cot Gores, J.; Zondag, H.A.; Schuitema, R.; van Helden, W.G.J., 2009b. Characterization of salt hydrates for compact seasonal thermochemical storage; presented at Effstock 2009.

van Essen, V.M., Bleijendaal, L.P.J., Kikkert, B.W.J., Zondag, H.A., Bakker, M., Bach, P.W, 2010. DEVELOPMENT OF A COMPACT HEAT STORAGE SYSTEM BASED ON SALT HYDRATES; presented at Eurosun 2010.

Zondag, H.A., van Essen, V.M., Bleijendaal, L.P.J, Kikkert, B.W.J., Bakker, M., 2010a. Application of MgCl2.6H2O for thermochemical solar heat storage; presented at IRES 2010.

Zondag, H.A., van Essen, V.M., Bakker, M., Bach, P.W., 2010b. An evaluation of the economical feasibility of seasonal sorption heat storage; presented at IRES 2010.

Zondag, H.A., Kikkert, B.W.J., Smeding, S., Bakker, M., 2011. Thermochemical solar heat storage with MgCl2.6H2O: first upscaling of the reactor; presented at International Conference for Sustainable Energy Storage 2011.